Developmental Biology 448 (2019) 59–68

Contents lists available at ScienceDirect

Developmental Biology

journal homepage: www.elsevier.com/locate/developmentalbiology

Insemination or phosphatidic acid induces an outwardly spiraling disk of elevated Ca^{2+} to produce the Ca^{2+} wave during *Xenopus laevis* fertilization

Colby P. Fees, Bradley J. Stith*

University of Colorado Denver, CO, USA

ARTICLE INFO

Keywords:
Fertilization
Phospholipase D
Phosphatidic acid
Intracellular calcium wave
Endoplasmic reticulum
Inositol 1, 4, 5-trisphosphate

ABSTRACT

During *Xenopus* fertilization, the initial intracellular calcium ($(Ca^{2+})_i$) release at the sperm-egg binding site (hot spot) has not been described without the use of inhibitors, nor related to underlying ER structure. Without inhibitors, we now report that sperm induce an initial hot spot after sperm addition to *Xenopus* eggs that was ~25 μm. This area is consistent with the size of ER patches and clusters of IP3 receptors that have enhanced activity. Furthermore, we find a new mechanism for the fertilization $(Ca^{2+})_i$ wave; instead of outward diffusion of inositol 1,4,5-trisphosphate (IP_3), we find that the wave was generated by an outward, clockwise rotation of a ~63 μm disk of elevated $(Ca^{2+})_i$ moving very rapidly at ~65 μm/s. We also suggest a new mechanism for the acceleration of the fertilization $(Ca^{2+})_i$ wave as the disk accelerated and was joined by other rotating disks (some rotating counterclockwise) at a time when the speed of the $(Ca^{2+})_i$ wave increases. To examine the role of phosphatidic acid (PA) in the release of $(Ca^{2+})_i$ during *Xenopus* fertilization, we find that two inhibitors of PA production delayed the appearance of fertilization hot spots by ~9–12 min but did not reduce the size of hot spots and actually accelerated the later $(Ca^{2+})_i$ wave. Surprisingly, global addition of PA to *Xenopus* eggs induced localized hot spots at a time and size that was similar to those induced after sperm addition. In contrast, sperm induce a rapid $(Ca^{2+})_i$ wave (~4 μm/s) within ~30 s after hot spot appearance, whereas hot spots induced by PA required an ~32 min to induce a very slow (~1 μm/s) $(Ca^{2+})_i$ wave with a lower peak of $(Ca^{2+})_i$. Thus, PA may not be required for the initial release of $(Ca^{2+})_i$ at the sperm-egg binding site, but mimics sperm by inducing a similarly sized localized $(Ca^{2+})_i$ release. As compared with sperm, PA may induce a weak, slow $(Ca^{2+})_i$ wave by slowly increasing IP3 receptor clustering. Addition of PA to *Xenopus* oocytes, or Ca^{2+} ionophore to either *Xenopus* oocytes or eggs, did not induce hot spots but a global $(Ca^{2+})_i$ wave that rapidly moved at ~12 μm/s.

1. Introduction

As in mammals, the *Xenopus* egg is arrested in metaphase II of meiosis and fertilization involves an isoform of phospholipase C (PLC) and the completion of meiosis. However, *Xenopus* fertilization involves activation of phospholipase D (PLD) to increase phosphatidic acid (PA) mass. PA binds and activates Src, which then phosphorylates and activates phospholipase C-gamma (PLCγ). This leads to phosphatidylinositol 4,5-bisphosphate (PI45P2) hydrolysis to inositol 1,4,5-trisphosphate (IP_3). IP_3 then binds to clustered IP_3receptors in the endoplasmic reticulum (ER) to induce the release intracellular calcium ($(Ca^{2+})_i$) and subsequent fertilization events (Bates et al., 2014; Busa et al., 1985; Fontanilla and Nuccitelli, 1998; Larabell and Nuccitelli, 1992).

With *Xenopus* fertilization, two different PLD inhibitors block the increase in PA mass, Src and phospholipase Cγ (PLCγ) activation, and 87% of the $(Ca^{2+})_i$ release (Bates et al., 2014). Similar to sperm, addition of PA to *Xenopus* eggs stimulated Src and PLCγ activity in the absence of increased $(Ca^{2+})_i$. In addition, PA increased IP_3 mass to levels achieved by sperm (twice that induced by Ca^{2+} ionophore), PLCγ translocation to rafts, and $(Ca^{2+})_i$ release (inhibited by IP_3 receptor blocker, but not by removal of extracellular Ca^{2+}) (Bates et al., 2014; Stith et al., 1994; Stith et al., 1994, 1997). As Src is already present in membrane rafts and PA does not alter the amount of Src in membrane rafts, we suggest that PA induces a conformational change to activate Src (Bates et al., 2014; Stith, 2015).

Abbreviations: Ca_i^{2+}, intracellular calcium; DAG, sn 1,2-diacylglycerol; dPA, 1,2- Dicapryloyl-*sn*-Glycero-3-Phosphate; dPS, 1,2-Dioctanoyl-sn-Glycero-3-[Phospho-L-Serine]; ER, endoplasmic reticulum; FIPI, 5-fluoro-2-indolyl des-chlorohalopemide; IP_3, inositol 1,4,5-trisphosphate; PA, phosphatidic acid; PI45P2, phosphatidylinositol 4,5-bisphosphate; PLC, phospholipase C; PLCγ, phospholipase C-gamma; PLD, phospholipase D; PS, phosphatidylserine

* Correspondence to: University of Colorado Denver, Department of Integrative Biology, Campus Box 171, PO Box 173364, Denver, CO 80217-3364, USA.
E-mail address: brad.stith@ucdenver.edu (B.J. Stith).

https://doi.org/10.1016/j.ydbio.2019.01.004
Received 5 September 2018; Received in revised form 3 January 2019; Accepted 4 January 2019
Available online 11 January 2019
0012-1606/

Sperm-egg binding triggers a localized release of $(Ca^{2+})_i$ (a "hot spot") but these hot spots have previously only been observed in the presence of Src, PLC, or IP_3 receptor inhibitors (Carroll et al., 1997; Fontanilla and Nuccitelli, 1998; Glahn et al., 1999; Runft et al., 1999; Stricker et al., 2010). We now provide new data on the generation of the hot spot without the use of inhibitors.

We also compare the initial $(Ca^{2+})_i$ release in the *Xenopus* egg and oocyte. The *Xenopus* oocyte is arrested in diplotene of prophase I of meiosis, cannot be fertilized and $(Ca^{2+})_i$ release is relatively transient with rapidly moving waves (up to ~23 μm/s). The $(Ca^{2+})_i$ wave in the oocyte is believed to be due to diffusion of $(Ca^{2+})_i$ to activate neighboring IP_3 receptors (Shuai et al., 2007; Ullah et al., 2014). In contrast, the *Xenopus* egg can be fertilized and has slow (~4–5 μm/s), prolonged $(Ca^{2+})_i$ waves involving higher levels of $(Ca^{2+})_i$ release (Machaca, 2004; Terasaki et al., 2001). One model for the fertilization $(Ca^{2+})_i$ wave in *Xenopus* is that IP_3 diffuses from the hot spot to a new site to release $(Ca^{2+})_i$ which then stimulates PLC to produce more IP_3 (Fall et al., 2004; Wagner et al., 1998; Wagner et al., 1998, 2004).

This change in the release of $(Ca^{2+})_i$ develops during oocyte maturation to the egg in both frog and mammalian species (Machaca, 2004; Ullah et al., 2014). It is largely due to extension of the endoplasmic reticulum (ER) into the cell cortex and the formation ER membrane "patches" with extensive membrane folding (Campanella and Andreuccetti, 1977; Chiba et al., 1990; El-Jouni et al., 2005; Kline, 2000; Stricker, 2006; Terasaki et al., 2001). The ER patches can be up to ~30 μm in diameter (my measurement from Fig. 5 in (Terasaki et al., 2001)) (Charbonneau and Grey, 1984; Kline, 2000; Sun et al., 2011). The cortical ER in the egg has large clusters of IP_3 receptors that are more sensitive to $[IP_3]$ (Boulware and Marchant, 2005; Machaca, 2004; Sun et al., 2011; Terasaki et al., 2001).

Without the use of Src, PLC or IP_3 receptor inhibitors, we find that the initial, local $(Ca^{2+})_i$ release in the hot spot involves the appearance of an outwardly rotating disk of elevated $(Ca^{2+})_i$ that generates the $(Ca^{2+})_i$ wave. The area of the initial release may be due to a cortical ER patch is similar in size to initial hot spots. Furthermore, the acceleration of the $(Ca^{2+})_i$ wave at 30–60 s noted by us and other labs may be due to the appearance of multiple rotating disks and the increase in the speed of the rotating disks. We suggest that that PA does not play a required role in this initial $(Ca^{2+})_i$ release as inhibiting PA production merely delays the appearance of the hot spots but does not affect their size. Instead, PA may facilitate an event prior to the initial $(Ca^{2+})_i$ release at the sperm-egg binding site, such as sperm-egg fusion. Inhibiting PA production led to an acceleration of the late $(Ca^{2+})_i$ wave perhaps by lowering peak $(Ca^{2+})_i$ or inhibiting the generation of multiple rotating disks. Mimicking sperm, addition of PA to *Xenopus* eggs induced hot spots of a similar diameter, a rotating disk and a very slow $(Ca^{2+})_i$ wave with lower peak $(Ca^{2+})_i$. These events may be induced by PA enhancement of the ER patches and IP_3 receptor clustering. In contrast to addition to eggs, PA addition to oocytes did not induce hot spots, but a global $(Ca^{2+})_i$ wave that moved ~12 times faster than the PA-induced wave in eggs.

2. Materials and methods

Wild type and albino *Xenopus laevis* frogs were obtained from *Xenopus* Express (Ft. Lauderdale, FL) or Nasco (Fort Atkinson, WI). Our animal care and protocols have been approved by the University of Colorado (IACUC #86617(12)1D). To obtain eggs, 3–4 days prior to use, females were primed with 35–50 IU pregnant mare serum gonadatropin (Sigma, St. Louis, MO.) and, to stimulate ovulation, subsequently injected with 800 IU of human chorionic gonadotropin 8–12 h before eggs were collected.

To obtain stage V and VI oocytes (average diameter of 1250 μm), frogs were primed with 35 IU pregnant mare's serum gonadotropin (PMSG) (Calbiochem) and, ~72 h later, ovaries were removed and placed into room temperature, modified O-R2 solution (83 mM NaCl, 1 mM $CaCl_2$, 1 mM $MgCl_2$, 10 mM HEPES, pH 7.8) (Stith et al., 1992). Cells were manually isolated from follicular membranes using watchmaker's forceps.

2.1. Intracellular calcium $(Ca^{2+})_i$ measurement

We used an inverted epi-fluorescent microscope to visualize intracellular $(Ca^{2+})_i$ release. We have published this method (Bates et al., 2014), but in brief, albino *Xenopus* eggs were placed directly onto a grid, treated for 2 min with injection solution (~10 ml of 10 mM Chlorobutanol, 82.5 mM NaCl, 20 mM $MgCl_2$, 10 mM HEPES, and 2 mM EGTA; pH 7.5) (Larabell and Nuccitelli, 1992; Sato et al., 1999), and after removal of the solution, eggs were microinjected with 4 nL of 10 mM Fluo-4 in 1.56:1 BAPTA:Ca^{2+}. To record relative changes in $(Ca^{2+})_i$ at fast recording rates (Darszon et al., 2004), we utilized Fluo-4 which shows a ~100 fold increase in fluorescence with Ca^{2+} binding.

After a second 2 min period in injection solution, cells were washed and rested for 30 min in 100% Modified Barth's Solution (MBS) (440 mM NaCl, 5 mM KCL, 50 mM HEPES, 4.1 mM Magnesium Sulfate Hydrate, 1.7 mM Calcium Nitrate Tetrahydrate, 2.1 mM $CaCl_2$, pH 7.5). PLD inhibitors, 5-fluoro-2-indolyl des-chlorohalopemide (FIPI) (Sigma-Aldrich or Caymen Chemical) or 1-butanol, was added for 30 min before eggs were washed (3 ×) and sperm added. Carrier DMSO was used as a control for FIPI, 2-butanol was used as a control for 1-butanol. In some experiments, 1,2-dicapryloyl-*sn*-glycero-3-phosphate (dicaproyl PA or dPA), 1,2-Dioctanoyl-sn-Glycero-3-[Phospho-L-Serine] (dPS) or calcium ionophore ionomycin (Sigma-Aldrich) was added (all lipids were from Avanti Polar Lipids, Alabaster, AL). To reduce the time required for agents to diffuse through the jelly coat, some eggs were partially dejellied after microinjection of calcium dye and a recovery period. Dejellying also prevented gravitational rotation after fertilization as the rotation of the cell would change the field of view during photography. Eggs were partially dejellied in 2% cysteine in MBS (pH 8) until the eggs almost touch each other (typically ~4 min) (Stith et al., 1994). The partially dejellied eggs were then washed four times before being exposed to agents. Partial dejellying did not affect the size of the $(Ca^{2+})_i$ release in response to PA (Bates et al., 2014). For fertilization of *Xenopus* eggs, testes were macerated in 2.4 ml of 100% MBS, and 167 μL of this sperm suspension (~10 million sperm) was added to eggs in 1 ml of 10% MBS (Stith et al., 1993).

An inverted Nikon Diaphot fluorescence microscope with an ORCA-ER digital camera recorded images every second in 2.1-grey scale that were analyzed by Simple PCI 6 software (Hamamatsu). Using individual images, we determined the center of the initial ~20 μm hot spot and measured out to the edge of the $(Ca^{2+})_i$ wave. This radius and the time of the image was used to calculate the speed of the wave. We also measured the initial diameter of the hot spot until the area of release extended over the edge of the viewing field (the rotating disk would extend the diameter twice in one 360° rotation).

As the saltatory increase in the radius of the hot spot correlated with the passing of the rotating disk, we also determined the time required for the disk to rotate around the entire circumference by recording the time to the next saltatory increase in the radius. Calculating the circumference of the hot spot, we determined the speed of the disk (μm/s). Furthermore, the saltatory extension of the radius was the rotating disk passed was a measure of the diameter of the rotating disk. We were able to follow more than one disk by marking events (passing of a disk with jump in radius) on a time line and continuing the established pattern of events for each disk).

We assembled the images into videos (Supplement) by exporting tif images from HCImage live and assembling them with FIJI/Image J. The videos can be viewed with VLC (version 2.2.6) which was superior to Windows Media player and, as monitor quality varies, contrast can be enhanced to view the rotating disk – especially at the top of the area of $(Ca^{2+})_i$ release: right click image, tools, effects/filters, video effects, check image adjust, to decrease contrast move slider to the right. For

Windows Media player, right click on the image/video, go to enhancement, video settings, move slider to the left ½, and decrease brightness by moving the slide over ¼. We did not modify the actual images but, in some cases, the contrast was decreased while viewing.

We calculated the relative $(Ca^{2+})_i$ increase by calculating in fluorescent intensity (F_{Ca}) divided by basal (F_o). To estimate actual $(Ca^{2+})_i$, calcium standards (Cal-BUF 1; World Precision Instruments, Sarasota, FL), ionic strength (http://www.lenntech.com/calculators/activity/activity-coefficient.htm) and MaxChelator (http://maxchelator.stanford.edu/) were used (Stith et al., 1994). With the standard line and an estimated cellular free volume of 0.56 µL (Stith et al., 1993), the actual amount of $(Ca^{2+})_i$ released was calculated.

At least three artifacts are associated with this method (Bates et al., 2014). Prior microjection of fluor can depolarize the egg membrane which inhibited sperm binding for up to 15 min (partially inducing a fast block to polyspermy). However, the average time of sperm-egg binding in our (~5.6 min) is similar to that reported by other labs using electrodes (~5 min) (Wozniak et al., 2018). Also, the fluor can act as a $(Ca^{2+})_i$ buffer and slow the $(Ca^{2+})_i$ wave, but our final estimated dye concentration of 71 µM was suggested to have minimal effect (Nuccitelli et al., 1993), the time of sperm-egg binding was similar to other reports, and our system is capable of recording waves up to at least 13 µm/s (see results with Ca^{2+} ionophore or PA addition to *Xenopus* oocytes; Table 2). Finally, as fertilization in *Xenopus* is believed to only occur in the pigmented animal pole, and since we used albino cells, the orientation of the cell was not known. Our data collection on $(Ca^{2+})_i$ release was limited to those sperm-egg binding sites (hot spots) occurring within our field of view (one half the zygote). Eggs that were fertilized at the edge of the field of view or on the other side were not included in our data collection. With our inverted microscope, the sperm were not able to fertilize at the center of the cell as it rested on the bottom of the dish. In addition, the edge of the egg was ~625 µm above the center of the egg which rested on the bottom of the dish. This difference in height could affect the level of fluorescence recorded and presented a problem with focusing (which was preset).

2.2. Statistics

All data in the text and figures are reported as average ± standard error of the mean (s.e.m.) and n is equal to the number of data points. Regression lines and the two-tailed Student's *t*-tests (in figures, significance at $P < 0.05$ was noted with an asterisk) were obtained with SigmaPlot (version 11.2, Systat Software, San Jose, CA, USA).

3. Results

We have reported a local $(Ca^{2+})_i$ release at the *Xenopus* sperm-egg binding site (Bates et al., 2014) and now present a detailed analysis. Insemination induced ~1.56 hot spots over the field of view (one half of the egg) (Table 1). The hot spots appeared at ~5.6 min after sperm addition, and a $(Ca^{2+})_i$ wave was apparent ~34 s later (~6.33 min after insemination) (Table 2). The wave then traveled from the sperm entry point across the egg at an average rate of ~4 µm/s (Table 1).

3.1. During Xenopus fertilization, an outwardly rotating disk(s) of elevated $(Ca^{2+})_i$ produced the fertilization $(Ca^{2+})_i$ wave

The first video (#1, Supplement) shows that sperm-egg binding "hot spots" can disappear and reappear. Without inhibitors, we can now describe in detail the size and shape of the first $(Ca^{2+})_i$ release located at 9 o'clock (middle, far left) that appeared at 7:40 min after insemination. A very faint signal appeared with a diameter of 20 µm, and 2 s later (7:42 min), this spot developed into a small vertical oval of elevated $(Ca^{2+})_i$ (64 µm vertical diameter, and a 36 µm horizontal diameter, or 64 × 36 µm). Two seconds later, at 7:44 min, the hot spot faded (50 × 36 µm), then the spot enlarged again to 107 × 57 µm at 7:46 min. At 7:50 min, the spot widened (107 × 72 µm), then faded again at 7:52 until it was undetectable by ~8:14 min (for a total duration of 34 s). As noted below, $(Ca^{2+})_i$ release reappeared in the same spot ~2 min later.

About 1.5 min after the first hot spot disappeared, a second sperm bound at 3 o'clock (far right of the cell) to induce a second hot spot at 9:36 min (27 µm vertical diameter). Over the next 2 s, the hot spot increased in size to a vertical diameter of 101 µm, disappeared by 9:48 min and did not reappear. This second event represented sperm induction of a transient (~12 s) local release of $(Ca^{2+})_i$ was unsuccessful in inducing a $(Ca^{2+})_i$ wave.

Based on marking the initial hot spot in Video #1, the hot spot at 9 o'clock reappeared 116 s after disappearance (10:10 min after insemination). To emphasize this successful sperm binding, we made two shorter videos (Video #2, close up Video #3, Supplement) which begin with this reappearance (changing to time in seconds from when the hot spot reappeared). The videos provided the best visual evidence that the expansion of the hot spot was found to be due to an outwardly rotating small disk of elevated $(Ca^{2+})_i$ that moved in a clockwise manner. After the initial hot spot faded at time 2 s, a bulge appeared at the lower right of the center, then there was an expansion at the lower left at 5 s, then the bulge appeared at 6 s to the upper left, then to the right at 7 s, then at the bottom of the hot spot at 8 s. At 9 s, there was an expansion to the

Table 1
Lowering PA levels with FIPI or 1-Butanol speeds the $(Ca^{2+})_i$ wave but does not alter the number or size of the hot spots. After insemination (Control), our $(Ca^{2+})_i$ imaging system recorded images that were analyzed for number and size of the local $(Ca^{2+})_i$ release at the sperm-egg binding site (the size of the hot spot was measured 30 s after initial appearance) and the speed of the subsequent $(Ca^{2+})_i$ wave (see Methods). Our results were limited to events occurring in one half of the egg/zygote (the field of view). Two inhibitors of PA production (FIPI or 1-butanol) were added before insemination (Bates, 2014). FIPI was dissolved in DMSO and diluted in MBS before addition to *Xenopus* eggs at the final concentration noted, and "DMSO" represents the carrier control group. The 1-butanol treatment groups were compared with 2-butanol (unable to inhibit PA production) groups. An asterisk denotes $p < 0.05$, and average ± s.e.m. are shown with group size designed by "n.".

	Control	DMSO	FIPI (µM)		
			0.1	**1**	**10**
Wave rate (µm/s)	4.06 ± 0.22 (n = 11)	3.95 ± 0.20 (n = 7)	*4.81 ± 0.22 (n = 7)	*4.83 ± 0.31 (n = 5)	*5.26 ± 0.31 (n = 7)
No. of hot spots/cell	1.56 ± 0.29 (n = 9)	1.57 ± 0.30 (n = 7)	1.86 ± 0.34 (n = 7)	2.33 ± 0.61 (n = 6)	2.14 ± 0.70 (n = 7)
Hot spot diameter (µm)	95 ± 3 (n = 18)	92 ± 1 (n = 5)	94 ± 1 (n = 5)	99 ± 3 (n = 10)	88 ± 3 (n = 7)

	Control	2-Butanol		1-Butanol		
		0.50%	**0.75%**	**0.25%**	**0.50%**	**0.75%**
Wave Rate (µm/s)	4.01 ± 0.14 (n = 18)	3.68 ± 0.05 (n = 3)	4.15 ± 0.20 (n = 4)	4.153 ± 0.21 (n = 4)	4.68 ± 0.32 (n = 3)	*4.59 ± 0.13 (n = 4)
No. of hot spots/cell	1.56 ± 0.29 (n = 9)	1.33 ± 0.33 (n = 3)	1.25 ± 0.25 (n = 4)	*2.5 ± 0.29 (n = 4)	3.67 ± 1.20 (n = 3)	*2.5 ± 0.29 (n = 4)

Table 2
Comparison of $(Ca^{2+})_i$ release as induced by addition of sperm or dPA With addition to *Xenopus* eggs (left two columns), this table compares the release of $(Ca^{2+})_i$ by dPA (1,2-dicapryloyl-*sn*-glycero-3-phosphate) and insemination. dPA induced spots of $(Ca^{2+})_i$ release on a time course similar to sperm, but the induction of a wave by dPA was much delayed, the dPA wave was slower with a lower peak $(Ca^{2+})_i$. The right two columns show data with *Xenopus* oocytes which lack egg jelly, ER patches and IP3 receptor clusters, and show transient faster $(Ca^{2+})_i$ waves. While experiments involved eggs from multiple different frogs over multiple days, typically, dPA and sperm were added to eggs from the same frog on the same day to facilitate a comparison. Values listed are the group average ± s.e.m. and group size listed as "n." An asterisk denotes P < 0.01.

	Added to *Xenopus* Eggs		Added to *Xenopus* Oocytes	
	Sperm	**dPA**	**dPA**	**Ca^{2+} Ionophore Ionomycin**
Time of first hot spot (min)	5.59 ± 0.43 (n = 11)	6.18 ± 0.69 (n = 3)	none	none
Number of hot spots per egg	1.56 ± 0.29 (n = 9)	3.00 ± 1.55 (n = 3)	none	none
Time of wave initiation after addition (min)	6.326 ± 0.44 (n = 11)	*38.20 ± 2.40 (n = 3)	1.64 ± 0.11 (n = 11)	0.39 ± 0.07 (n = 9)
Wave rate (μm/s)	4.06 ± 0.22 (n = 11)	*1.04 ± 0.03 (n = 3)	13.2 ± 0.7 (n = 3)	12.5 ± 0.5 (n = 3)
Maximum fluorescence (F_{Ca}/F_o)	1.96 ± 0.09 (n = 11)	*1.66 ± 0.05 (n = 3)	1.54 ± 0.06 (n = 11)	2.35 ± 0.08 (n = 6)

left, at 10 s an expansion to the upper left and this pattern of rotating expansion continued to the 20 s image. Note that the rotation is along the edge of the area where $(Ca^{2+})_i$ already has been released and the disk does not rotate beyond this edge or into the area of prior $(Ca^{2+})_i$ release.

To provide quantification of the qualitative description of the rotation, we measured the vertical and horizontal right radii (Fig. 1A and inset, respectively) along with the vertical diameter (Fig. 1B). The initial area of $(Ca^{2+})_i$ release was circular with a radius of ~18 μm (time set to 1 s in Fig. 1 and Video #2). In the next second (at 2 s after appearance), the spot narrowed (horizontal radius decreased to 9 μm), and at 3 s, the vertical radius increased to 36 μm while the horizontal radius increased back to 18 μm (a bulge appeared at the lower right of the center). At 4 s, the vertical radius decreased to 18 μm and the horizontal radius decreased to 9 μm. At 5 s, the vertical radius again jumped back to 38 μm while the horizontal radius returned to 18 μm (i.e., expanded to the lower left). At 6 s, there was an expansion to the upper left with the vertical radius at 39 μm, and the horizontal radius increased to 36 μm. At 7 s, there was an expansion to the upper right (vertical diameter of 55 μm, horizontal radius of 45 μm). The vertical diameter remained at ~55 μm from 7 s to 9–10 s. At 11–13 s, the vertical radius jumped to ~75 μm, with the horizontal radius increased to ~52 μm.

The vertical diameter of the hot spot (Fig. 1B) also shows a jump in the diameter as the disk passes either the top or bottom of the hot spot. Cartoons were added to Fig. 1B to highlight the position of the rotating disk during each plateau of the increase in the diameter of the hot spot (after the disk passed, the location of the edge of the hot spot was stable). Using the time between saltatory jumps (time required for the rotating disk to move 360°), the circumference of the hot spot, and the increase in diameter as the rotating disk passed, the size of the rotating disk was 63 ± 1.4 μm (n = 7) and it moved at an average speed of 65 ± 1.8 μm/s (n = 12) in an outward spiral to generate the $(Ca^{2+})_i$ wave. For example, one rotating disk took ~9 s to rotate 360° along the edge of a circle of $(Ca^{2+})_i$ release with a radius of 93 μm, or a circumference of 584 μm (velocity = 584 μm/9 s).

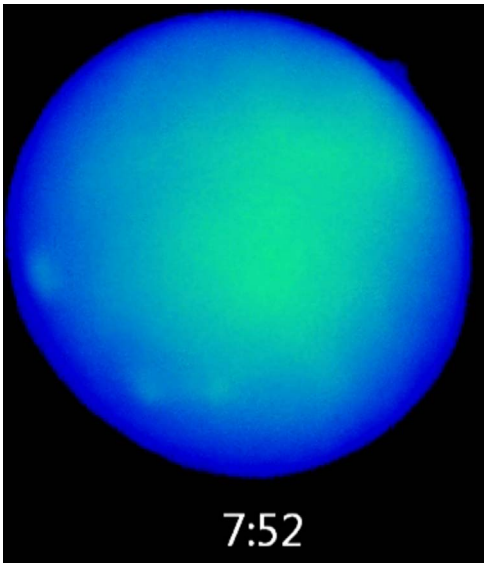

Video S1. *Xenopus* fertilization with sperm added at time zero and three hot spots are shown: one sperm bound at 9 o′clock, disappeared, a second sperm bound at 3 o′clock and disappeared and there was a reappearance of a hot spot at the original 9 o′clock site. Time (in minutes) is from the point of insemination. For scale, the average *Xenopus* egg diameter was 1250 μm, and that the wave duration in control fertilization was 4.95 ± 0.37 min (n = 11). Of the commonly available free video viewers, we recommend VLC (https://www.videolan.org/vlc/). If desired, to enhance the image of the rotating disk: right click image, tools, effects/filters, video effects, check image adjust, to decrease contrast move slider to the right. For Windows Media player: right click on the image/video, go to enhancement, video settings, move slider to the left to decrease contrast, or decrease brightness setting). A video clip is available online.Supplementary material related to this article can be found online at doi:10.1016/j.ydbio.2019.01.004.

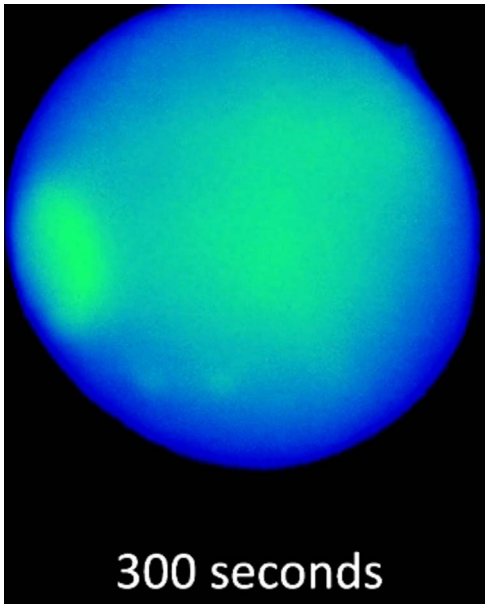

Video S2. To emphasize the rotating disk, Video #2 shows only one hot spot leading to a (Ca2 +)i wave and is a shorter version of video #1. Video #2 starts at second appearance of the (Ca2 +)i release at 9 o′clock, and the time scale for video #2 was altered so that time zero is the time of the original appearance at the 9 o′clock site. In this video, the second, successful appearance is at 210 s after original hot spot appearance. For scale, the average *Xenopus* egg diameter was 1250 μm. Of the commonly available free video viewers, we recommend VLC (https://www.videolan.org/vlc/). If desired, to enhance the image of the rotating disk: right click image, tools, effects/filters, video effects, check image adjust, to decrease contrast move slider to the right. For Windows Media player: right click on the image/video, go to enhancement, video settings, move slider to the left to decrease contrast, or decrease brightness setting).Supplementary material related to this article can be found online at doi:10.1016/j.ydbio.2019.01.004.

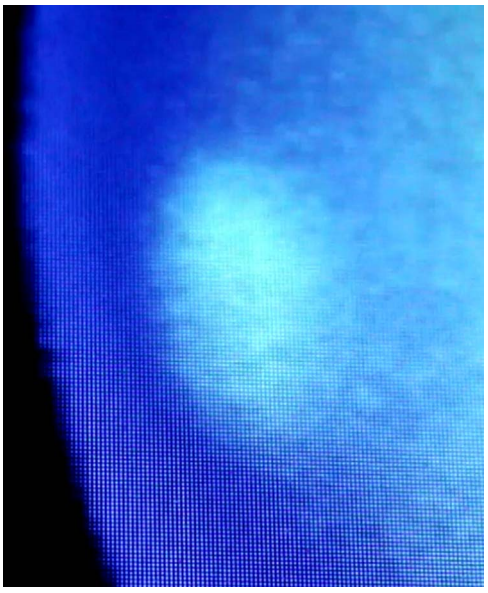

Video S3. a close-up of the initiation of the hot spot and rotating disk (taken from video #2). For scale, the average *Xenopus* egg diameter was 1250 µm. Of the commonly available free video viewers, we recommend VLC (https://www.videolan.org/vlc/). If desired, to enhance the image of the rotating disk: right click image, tools, effects/filters, video effects, check image adjust, to decrease contrast move slider to the right. For Windows Media player: right click on the image/video, go to enhancement, video settings, move slider to the left to decrease contrast, or decrease brightness setting). Supplementary material related to this article can be found online at doi:10.1016/j.ydbio.2019.01.004.

As identified in Fig. 1A, a second clockwise-rotating disk arose by ~26 s followed by a third counterclockwise-rotating disk, and the saltatory increases in radius began to disappear at ~26 s (Fig. 1; Video #2). This disappearance of steps due to the appearance of multiple rotating $(Ca^{2+})_i$ disks occurred in another experiment at ~55 s after hot spot appearance (Fig. 4). When the wave was halfway across the zygote (~16 min from insemination, noted in Video #1), rotating disks (bulges) can still be seen rotating (best noted at the top edge of the $(Ca^{2+})_i$ wave). Thus, the rotating disk became harder to detect, the disks were still present in later stages of the $(Ca^{2+})_i$ wave.

We also found two, long lasting areas of higher $(Ca^{2+})_i$ that were present before insemination. With an ~80 µm diameter (similar in size to sperm induced hot spots), they were located at 7 o'clock and 6:30 o'clock in Video #1. As the $(Ca^{2+})_i$ wave approached these areas, the wave moved rapidly moved into these areas to form a projection from the uniform wave front (there was no inhibition of the movement of the wave through these hot spots). We did not observe any sperm binding in these areas. These stable areas of slightly higher $(Ca^{2+})_i$ may represent areas of ER patches with higher IP_3 receptor density (see Discussion).

3.2. Speed of the rotating disk and the acceleration of the $(Ca^{2+})_i$ wave

While the average speed of the rotating disk of $(Ca^{2+})_i$ was 65 µm/s, combining data from experiments, we noted that the disk speed actually increased (Fig. 2). From an initial speed of 57 ± 1.5 µm/s (n = 11), at 55 s after hot spot appearance (hot spot diameter ~320 µm), the rotating disk sped up to 80 ± 4.8 µm/s (n = 6). The speed may change due to reaching a critical diameter of the hot spot or that the presence of multiple rotating disks may accelerate the disks (multiple disks arose as early as ~26 s or 240 µm after hot spot appearance).

The initial speed of the $(Ca^{2+})_i$ wave was 3.45 ± 0.16 µm/s (n = 16; a range of 2.3–4.3), after ~40 s (~200 µm hot spot diameter), the speed increased by 17% ($p < 0.03$) to 4.03 ± 0.16 µm/s (n = 18; a range of

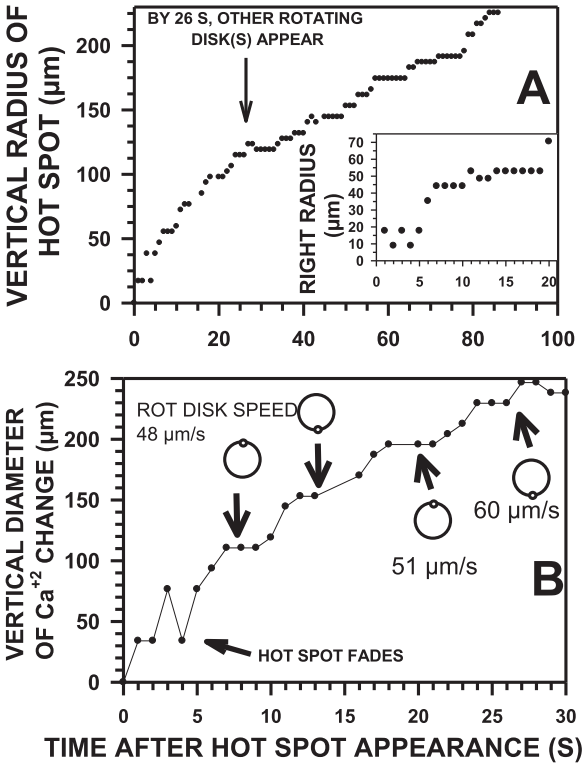

Fig. 1. During *Xenopus* fertilization, the initial site of $(Ca^{2+})_i$ release increases in a saltatory manner. Using our videos (Supplement), changes in the radius of the hot spot are consistent with the passing of a rotating disk of elevated $(Ca^{2+})_i$ that produces the $(Ca^{2+})_i$ wave in *Xenopus* fertilization. (A) We first measured the radius of the hot spot in two directions to obtain a measure of the rotation of the release of $(Ca^{2+})_i$. The large Y axis is the vertical radius measured from the center of the hot spot (presumptive sperm-egg binding site) upward, while the Y axis in the inset is the radius from the center to the right edge of the area of elevated $(Ca^{2+})_i$. The X axes in panels A and B represent the time of the second appearance of this hot spot at the 9 o'clock position (in Video #1, at 10:10 min:s after insemination). (B) To examine the speed of the rotating disk of $(Ca^{2+})_i$, we then measured the vertical diameter (Y axis). As the rotating $(Ca^{2+})_i$ disk passed either the top or bottom of the hot spot, there was a jump in the diameter. The cartoons use a large circle to represent the hot spot and a small circle to represent the position of the rotating disk at specific jumps in the diameter. The speed noted under the cartoons was the speed of the rotating disk at that specific point (see Methods).

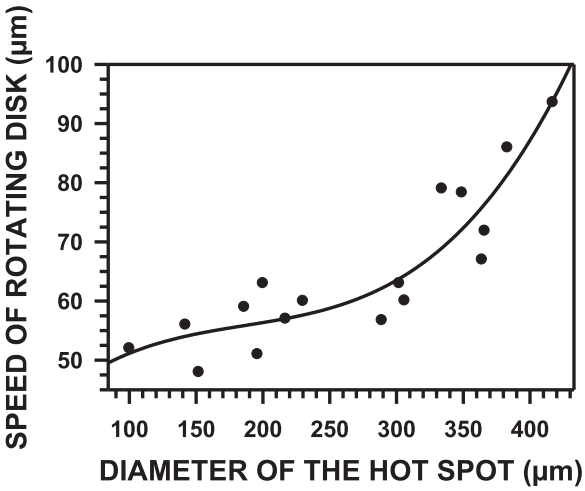

Fig. 2. The speed of the rotating disk of elevated $(Ca^{2+})_i$ increases when the hot spot diameter reaches ~350 µm. As the $(Ca^{2+})_i$ wave is due to a rotating disk of elevated $(Ca^{2+})_i$, we determined the speed of a disk over time after the localized $(Ca^{2+})_i$ release began (see Methods section). A third order quadratic equation describes the increase in disk speed: $y = 0.290 \times - 0.001362 \times^2 + 0.000002431 \times^3 + 33.3$; $r^2 = 0.833$).

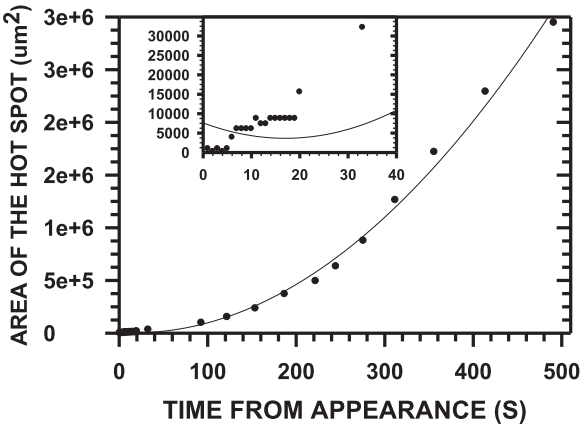

Fig. 3. The area of the $(Ca^{2+})_i$ release is found to increase exponentially. With the ability to visualize the center of the initial, small (20 μm) site of $(Ca^{2+})_i$ release, we calculated the area of the $(Ca^{2+})_i$ release from images of $(Ca^{2+})_i$ release during *Xenopus* fertilization from the time of the appearance of the successful sperm-egg interaction (hot spot) to ~8 min later. The insert highlights the early saltatory increase due to one rotating disk. The data are described by a third order equation (exponential modeling was not as accurate): area of $(Ca^{2+})_i$ release per second ($\mu m^2/s$) = (-466.0)X + 13.69 $\times^2$ + 7623 (r^2 = 0.995).

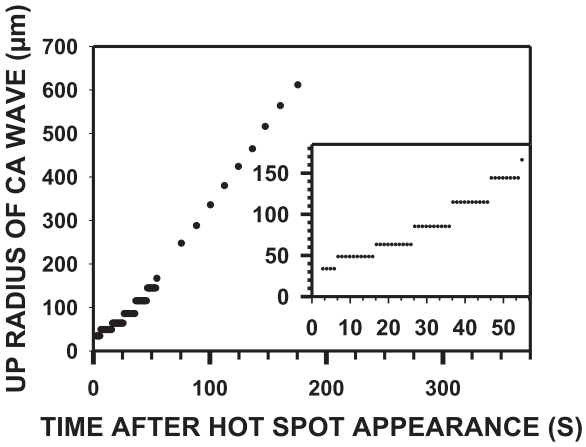

Fig. 4. A second example of the saltatory increase in the growth of the radius of the area of $(Ca^{2+})_i$ release during *Xenopus* fertilization. As compared with the experiment shown in Fig. 1, in this experiment, the vertical radius was recorded over a longer time period, and secondary rotating disks arose later (~55 after hot spot appearance). The inset highlights the early saltatory increase in hot spot radius when only the initial clockwise rotating disk was present.

3.2–5.17). As the increase in the wave speed occurred when multiple rotating disks appear (25–60 s) and when the disks accelerate (~55 s), the speeding of the $(Ca^{2+})_i$ wave may be due to these two factors. That is, the acceleration may not be to a change in wave mechanism as has been suggested, but an enhancement of one mechanism involving the rotating disk(s).

As we can record the initial hot spot to pin point the center, we can now accurately report the increase in the area of $(Ca^{2+})_i$ release over time (Fig. 3). The rate of the increase in the area of the hot spot is described by a third order equation (exponential modeling was not as accurate): area of $(Ca^{2+})_i$ release per second ($\mu m^2/s$) = (-466.0)X + 13.69 $\times^2$ + 7623 (r^2 = 0.995). Over the time period of 20–93 s after hot spot appearance, the area increased at a rate of 1110 $\mu m^2/s$ (r^2 = 0.999). Between 93 and 245 s, the rate further increased to 3501 $\mu m^2/s$ (r^2 = 0.975), and from 276 to 491 s the rate was 9643 $\mu m^2/s$ (r^2 = 0.998).

In a different experiment, a hot spot appeared at 448 s after insemination along the edge of the zygote (Fig. 4). With hot spot appearance set to 1 s, the radius remained at 33 μm from 1 to 4 s, however the hot spot became brighter. At 4 s, the radius jumped to 48 μm, at 15 s to 63 μm, at 25 s to 84 μm, and at 35 s to 114 μm. The first disk rotated clockwise and at 53 s, a second disk arose that rotated counterclockwise. Over the first ~40 s, the wave rate was 1.7 μm/s, and then it increased to 3.5 μm/s. The speed of the rotating disks increased over this time (39, 52, 72, 90 μm/s) and had an average speed of 72.3 ± 7.8 μm/s (s.e.m., n = 4).

3.3. Lowering PA levels only delays the hot spot appearance, but speeds the $(Ca^{2+})_i$ wave

To examine the mechanism of the fertilization $(Ca^{2+})_i$, we inhibited phosphatidic acid (PA) production and recorded $(Ca^{2+})_i$. In *Xenopus* fertilization, two PLD inhibitors (FIPI and 1-butanol, with 2-butanol control) prevent PA mass increase, Src and PLCγ activation, and blocked 87% of the total $(Ca^{2+})_i$ release (Bates et al., 2014). Yet, these inhibitors only delay the appearance of a diminished $(Ca^{2+})_i$ wave, gravitational rotation and first cleavage by ~9 min (FIPI) or 12 min (1-butanol) (Bates et al., 2014).

We now report that the two PLD inhibitors also delayed the appearance of hot spots by ~8.4 min (from 5.6 ± 0.4– to 14.0 ± 0.5 min, n = 7 and 17, respectively, p < 0.001). Although delayed, FIPI did not alter the size of the hot spots (Table 1)

In addition to delaying the onset of hotspots, the two PLD inhibitors actually accelerated the average speed of the diminished $(Ca^{2+})_i$ wave (Table 1). In control fertilization, the average wave speed was 4.05 μm/s (n = 29), and the PLD inhibitors increased the average speed of the wave by ~30% (to 5.26 μm/s) for FIPI, or ~15% (to 4.59 μm/s) for 1-butanol. In another comparison, we combined the two control groups (n = 18) and the three FIPI treatment groups (n = 19); comparison of these two large groups show that FIPI accelerated the Ca wave by 27% (p < 0.001).

As noted above, the fertilization $(Ca^{2+})_i$ wave accelerated at ~30–60 s after hot spot appearance, however, lowering PA with FIPI did not change the speed of the initial slow $(Ca^{2+})_i$ wave (control: 3.45 ± 0.16, n = 16; FIPI treated: 3.77 ± 0.24 μm/s, n = 20; p < 0.3). Thus, PA does not affect the speed of the disk. In contrast, after ~60 s, FIPI increased the speed of the wave so lowering PA may stimulate the appearance of multiple disks (i.e., elevated PA may inhibit the appearance of new rotating Ca^{2+} disks). This suggestion is consistent with the fact that addition of PA induced a slow $(Ca^{2+})_i$ wave that did not accelerate (Section 3.5).

3.4. PA levels may not play a role in the local $(Ca^{2+})_i$ release at the sperm-egg binding site (hot spots)

One might expect that the ~9–12 min delay in the appearance of hot spots, as induced by the PLD inhibitors, would allow for more sperm to bind the egg. Restated, a delay in the block to polyspermy would produce additional hot spots. However, while there was a trend toward an increase in the presence of FIPI, this was not significant (Table 1). Even after combining the control and DMSO treated groups (1.56 ± 0.3, n = 16) and the two highest [FIPI] treatment groups (2.24 ± 0.65, n = 13), no significant difference between the two combined groups was found (P < 0.321).

However, the other PLD inhibitor 1-butanol did increase the number of hot spots (Table 1). As we did with FIPI, we combined all control groups, and compared this group to all 1-butanol treated groups. 1-butanol increased the number of hot spots from 1.44 ± 0.18 per cell (n = 16) to 2.5 ± 0.17 (n = 11; p < 0.001) – an increase of 74%. Based on our earlier work (Bates et al., 2014), this increase in hot spots may be due to 1-butanol inhibition of exocytosis and the late block to polyspermy (FIPI does not have this non-specific effect).

As the two PLD inhibitors did not affect the size of the hot spots or the movement of the initial rotating $(Ca^{2+})_i$ disk, PA may not play a required role in the initial $(Ca^{2+})_i$ release at the sperm binding site. Since the PLD inhibitors only delayed hot spot appearance, PA may

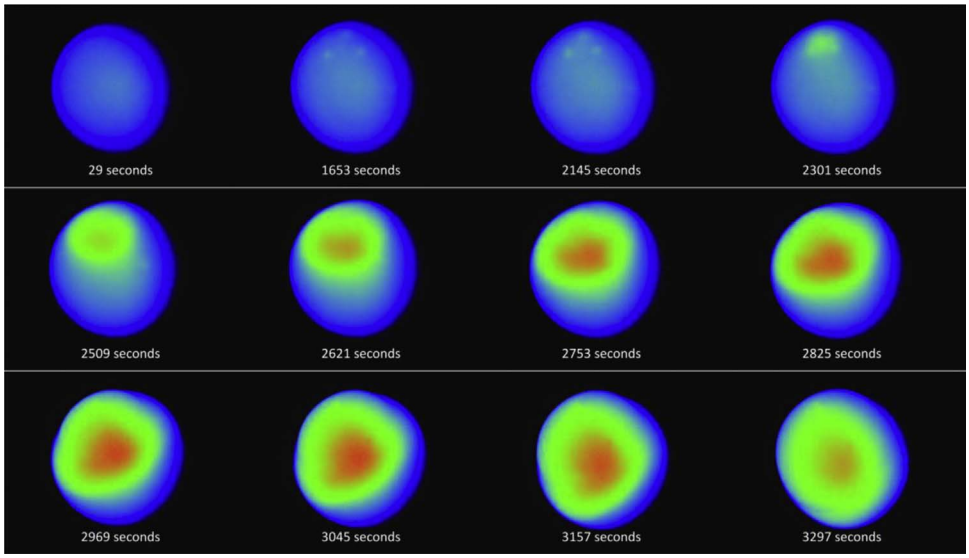

Fig. 5. $(Ca^{2+})_i$ release after addition of dPA to a *Xenopus* egg. Dicaproyl phosphatidic acid (dPA) was added at time zero and induced 3 spots of elevated $(Ca^{2+})_i$ at ~6 min. The spots were long lasting: see hot spots in images at 1653 s or 27.55 min; and at 2145 s or 35.75 min. A $(Ca^{2+})_i$ wave initiated at ~38 min (see image at 2301 s after dPA addition). dPA was present over the entire period at 400 μM as this is the concentration required for maximal PA activation of fertilization events (half maximal response at ~150 μM)(Bates et al., 2014).

play a role in an earlier event such as sperm-egg membrane fusion.

3.5. Addition of PA to Xenopus eggs induces hot spots and a weak, slow $(Ca^{2+})_i$ wave

Addition of PA to eggs leads to activation of fertilization events such as Src and PLCγ activation, translocation of PLCγ to rafts, cortical contraction, gravitational rotation (a measure of cortical granule exocytosis) and $(Ca^{2+})_i$ release (the latter is blocked by IP_3 receptor blocker 2-APB, but not by removal of extracellular Ca^{2+}) (Bates et al., 2014).

To address the mechanism of hot spot generation, we added PA to eggs and found $(Ca^{2+})_i$ hot spots that arose at the same time as sperm (~6 min after addition; Table 2), and the hot spots were of similar size (PA: 81 ± 11 μm, n = 3; vs. 95 ± 3 μm, n = 18, for sperm). However, the PA induced spots were longer lasting (~32 min) and had diminished $(Ca^{2+})_i$ release as compared to hot spots induced by sperm (Table 2). As a solution of PA bathes the egg in a uniform manner (we did not add PA directly against the egg surface), one would expect a global release of $(Ca^{2+})_i$. In fact, a global $(Ca^{2+})_i$ release was seen after addition of PA to oocytes or Ca^{2+} ionophore addition to eggs (Section 3.6).

In the experiment shown in Fig. 5, PA addition resulted in three spots of elevated $(Ca^{2+})_i$ and a wave (in other PA experiments, coalescing of spots was not observed). The $(Ca^{2+})_i$ wave traveled across the egg over the next 23 min at 0.9 μm/s and this was followed 3.1 min later by a wave of surface contraction.

The PA-induced hot spots in eggs were capable of generating a rotating disk and a diminished, very slow wave (1 μm/s; Table 2). The hot spots appeared at ~6 min after addition of PA and it was another ~32 min before a wave initiated (successful sperm induce waves by ~30 s after hot spot appearance). Not only was the speed of the wave induced PA only ~25% of the speed of the wave induced by sperm (Table 2), but there was no acceleration of the PA-induced wave as found after insemination.

In a another comparison of PA and sperm action, the total cellular $(Ca^{2+})_i$ release by the two methods were graphed together (Fig. 6). Sperm produced a large elevation of $(Ca^{2+})_i$ from ~5–28 min with the wave requiring only 5.0 ± 0.4 min (n = 11) to travel from the hot spot to the antipole. In comparison, PA produced a lower elevation of $(Ca^{2+})_i$ from ~36–66 min and a slower wave that required 17.4 ± 0.9 min (n = 3) to travel to the antipole. In the Discussion, we suggest that PA may be enhancing ER patching and IP_3 receptor clustering over this ~32 min time period to induce a $(Ca^{2+})_i$ wave.

3.6. Addition of PA, PS or Ca^{2+} ionophore to Xenopus oocytes

As compared with eggs (see Introduction), *Xenopus* oocytes have very little IP_3 receptor clustering and demonstrate very fast but transient $(Ca^{2+})_i$ waves. Perhaps due to the lack of egg jelly or permeability differences, PA addition to *Xenopus* oocytes required only ~1.6 min after addition to induce a global $(Ca^{2+})_i$ release (no hot spots were found) (Table 2). PA addition to oocytes elevated $(Ca^{2+})_i$ to levels similar that induced by PA addition to eggs, but less than that induced by insemination or Ca^{2+} ionophore (Table 2). With oocytes, PA induced a very fast $(Ca^{2+})_i$ wave (~13 μm/s) that probably involves $(Ca^{2+})_i$ diffusion to activate the next IP3 receptor (not IP3 production and diffusion as in the egg).

In contrast to PA or sperm, Ca^{2+} ionophore ionomycin addition to *Xenopus* oocytes or eggs did not induce hot spots but a global release. With oocytes, ionomycin induced a very fast wave (~12.5 μm/s) and the largest $(Ca^{2+})_i$ release (Table 2). While PA induced a half maximal $(Ca^{2+})_i$ release at 5.78 ± 0.17 min (n = 11) and a maximal release by 10.04 ± 0.28 min (n = 11), ionomycin was faster with half-maximal and maximal responses at 1.24 ± 0.23 min (n = 6) and 5.94 ± 0.51 min (n = 6).

Addition of another anionic lipid, 1,2-Dioctanoyl-*sn*-Glycero-3-[Phospho-L-Serine], did not release $(Ca^{2+})_i$ in eggs or oocytes.

4. Discussion

4.1. The release of $(Ca^{2+})_i$ at the sperm binding site ("hot spot")

The local $(Ca^{2+})_i$ release at the sperm-egg binding site has not been viewed with the use of inhibitors of enzymes or the IP_3 receptor. However, without inhibitors, we now report that the sites of sperm-egg interaction (hot spots) can appear, disappear and reappear. The initial detectable area of $(Ca^{2+})_i$ release was a very faint small area (25 ± 3.4 μm diameter, n = 4), that immediately began rotating clockwise. The average diameter of elevated $(Ca^{2+})_i$ increased to a diameter of 63 μm, began rotating clockwise and, after 25–60 s (200–300 μm hot spot diameter), the initial rotating disk was joined by other similarly sized disks (some rotating counterclockwise). There was an increase in the speed of the rotating disks (from 57 to 80 μm/s) at this time. The

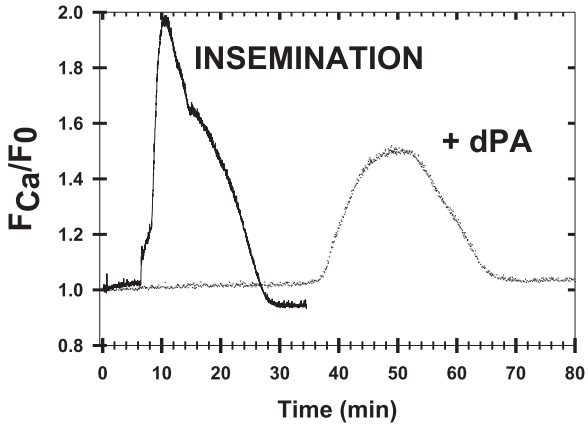

Fig. 6. A comparison of the increase in total $(Ca^{2+})_i$ during *Xenopus* fertilization and after dPA addition. The maximal change in fluorescent intensity (F_{Ca}) over basal (F_o) (measured over the entire egg/zygote) was graphed versus time after sperm or dPA (400 μM) addition. Images were captured at 1 per s (fertilization) or 2 per s (dPA). Due to their small $(Ca^{2+})_i$ release, prior hot spots are not visible in this figure, and the increase shown represents the large release during and after the $(Ca^{2+})_i$ waves.

$(Ca^{2+})_i$ wave also accelerated at this time (from 3.5 to 4 μm/s) so the increase in the number of rotating disks and their acceleration may be responsible. Thus, as opposed to past suggestions, the mechanism of the $(Ca^{2+})_i$ wave does not appear to change, but there is an enhancement of one mechanism (rotating disks) that results in the acceleration of the fertilization $(Ca^{2+})_i$ wave.

As described in the Introduction, cortical ER patches that contain clustered IP_3 receptors increase during oocyte maturation to the egg. Clustered IP3 receptors are geometrically sensitized to produce the long lasting, high $(Ca^{2+})_i$ release shown in eggs and the slow moving wave after fertilization (Charbonneau and Grey, 1984; Kline, 2000; Sun et al., 2011). These ER patches have been shown to be up to ~20 μm in diameter (e.g., Fig. 5; (Machaca, 2004)), which is consistent with the area of the initial $(Ca^{2+})_i$ release at the sperm binding site (hot spot) described here. Also, in some cells, we noted areas of slightly elevated $(Ca^{2+})_i$ that were present before insemination, were long lasting, and of similar size to those induced by sperm or PA. These areas may reflect areas in which cortical ER patches are more active or have more clustered IP_3 receptors.

4.2. Hot spots generated after use of inhibitors

IP3 and its receptor may not be required for the initial $(Ca^{2+})_i$ release but the subsequent $(Ca^{2+})_i$ wave. This is based on use of low levels of an IP_3 receptor blocker, heparin, as subsequent insemination of *Xenopus* eggs produced hot spots that lasted ~5–6 min and were ~77 ± 6 μm (n = 3; my estimate from published images (Fontanilla and Nuccitelli, 1998)). In contrast, we noted that sperm induce hot spots that typically last for less than 30 s whereas PA-induced hot spots that lasted 30 min or more. Under certain conditions, heparin did not inhibit hot spot generation but inhibited the $(Ca^{2+})_i$ wave so the authors suggested that different mechanisms of $(Ca^{2+})_i$ release are involved in the generation of hot spots versus waves (Fontanilla and Nuccitelli, 1998). In some cases with heparin, insemination induced a lower peak of $(Ca^{2+})_i$ with a very slow wave (similar to PA, as low as 1.9 μm/s) that often did not reach the antipole. In related experiments, an inhibitory IP_3 receptor antibody prevented the $(Ca^{2+})_i$ wave but not hot spots after insemination of *Xenopus* eggs (Fontanilla and Nuccitelli, 1998; Runft et al., 1999). As shown in their Fig. 4, row B (Runft et al., 1999), multiple hot spots appeared and they all disappeared in less than ~40 s (versus the longer lasting hot spots with the other IP_3 receptor blocker, heparin). By my measurements, the hot spots presented in their photos had a height of 112 ± 5 μm and a width of 78 ± 5 μm (s.e.m., n = 4 each).

Src plays a role in *Xenopus* fertilization but the tyrosine kinase inhibitor lavendustin A did not inhibit hot spots but could inhibit the $(Ca^{2+})_i$ wave: at ~7 min after insemination a hot spot of ~100–200 μm appeared, lasted for ~42 s, but no wave was observed (Glahn et al., 1999). Subsequently, a second hot spot arose at ~10.5 min and generated a very slow wave. Thus, sperm induce a slow wave after lavendustin A or heparin, or by PA addition alone. Although we find a delay in hot spot appearance with inhibition of PA production, lavendustin A did not alter the average time from insemination to the first rise in $(Ca^{2+})_i$ (~6 min). This suggests that tyrosine kinase activity is not needed for the initial release of $(Ca^{2+})_i$ but may be needed for the $(Ca^{2+})_i$ wave. Furthermore, hot spots produced in lavendustin A-injected eggs lasted about as long as those in the presence of the IP3 receptor antibody, but did not last as long as those seen in fertilized heparin-injected eggs (Glahn et al., 1999) or after PA addition.

With fertilization in the protostome worm *Cerebratulus*, the PLC inhibitor U73122 did not block hot spots (~22 μm diameter, similar to our initial hot spot size) but did block the $(Ca^{2+})_i$ wave (Stricker et al., 2010). In starfish egg fertilization (Carroll et al., 1997), inhibition of PLCγ produced hot spots that were ~85 μm in diameter and then spread to ~136 μm before disappearing by ~15 s.

Thus, PA (Section 4.4 below), tyrosine kinase and PLC activity, or the IP_3 receptor does not block the initial release of $(Ca^{2+})_i$ at the sperm binding site, but they may play an important role in the subsequent $(Ca^{2+})_i$ wave.

4.3. $(Ca^{2+})_i$ release in Xenopus eggs versus oocytes

The outward spiral pattern of the rotating disk of $(Ca^{2+})_i$ release at fertilization is reminiscent of a spiral pattern of $(Ca^{2+})_i$ release induced with IP_3 in *Xenopus* oocytes (Lechleiter et al., 1991) (http://parkerlab.bio.uci.edu/images_movies_presentations/calcium.htm). The narrow (width of ~40 μm, similar in scale to our hot spot) oocyte $(Ca^{2+})_i$ wave is due to IP3 bound IP3 receptors and Ca^{2+}-induced Ca^{2+} release (CICR). In CICR, $(Ca^{2+})_i$ released through one IP3 receptor/channel would diffuse and bind nearby IP3 receptors to stimulate them. The $(Ca^{2+})_i$ wave appeared to be a spiral due to adjacent areas located closer to the center that have very high $(Ca^{2+})_i$ that inhibit IP_3 receptors (refractory receptors). The opposite side of the narrow area of $(Ca^{2+})_i$ release has low $(Ca^{2+})_i$ with "resting" IP3 receptors. The spirals required 5.5 s for each rotation, and were transient (lasting ~33–44 s) (Girard et al., 1992). With CICR, the oocyte $(Ca^{2+})_i$ wave has speeds up to 23 μm/s.

As opposed to the oocyte, the *Xenopus* egg has larger clusters of IP_3 receptors to induce a "geometric sensitization" of IP_3 receptors (clustered receptors are sensitive to lower $[IP_3]$). In addition, the closeness of the IP_3 receptors means that release of $(Ca^{2+})_i$ by one receptor would produce high levels of $(Ca^{2+})_i$ to inhibit nearby IP_3 receptors and produce a much slower wave (4–9 μm/s) (Ullah et al., 2014). Instead of CICR, the fertilization wave is believed to be due to the diffusion of IP_3 to stimulate $(Ca^{2+})_i$ release to activate PLC (Larabell and Nuccitelli, 1992) to provide further IP_3 production (Bugrim et al., 2003; Fall et al., 2004; Wagner et al., 2004).

As noted, with *Xenopus* eggs, the diameter of the initial area of $(Ca^{2+})_i$ release (hot spots) was ~25 μm, with rotating disks of 63 μm, and these numbers can be compared to $(Ca^{2+})_i$ "puffs" in the oocyte. An oocyte puff involves activation of a cluster of up to ~50 IP_3 receptors over an area up to ~0.8 μm wide, which produces a $(Ca^{2+})_i$ release over an area ~5–10 μm wide (Dargan and Parker, 2003; Machaca, 2004; Shuai et al., 2006). With increased IP3 receptor clustering in the egg, one would expect the larger areas of $(Ca^{2+})_i$ release (e.g., 25–63 μm). In addition, the very rapid 65 μm/s movement of the rotating disk in the egg might involve a jump from one IP3 receptor cluster to the next due to CICR at the front of the disk (not diffusion of IP_3, or a wave of PLC activation). The rotating disk did not move into the cytoplasm away from the edge of the hot spot perhaps due to limited $(Ca^{2+})_i$ diffusion:

that is, the side of the disk that faces the cytoplasm would not extend beyond ~63 μm from the prior area of $(Ca^{2+})_i$ release (hot spot). The rotating disk may not reenter the area of elevated $(Ca^{2+})_i$ due to refractory IP_3 receptors present there. The orientation of the IP3 receptor channel may relate to why the initial disk rotated clockwise: the efflux of Ca^{2+} from the ER store may be oriented in this forward direction.

4.4. Role of PA in the initial $(Ca^{2+})_i$ release or hot spot

In *Xenopus* fertilization, sperm activate PLD to produce PA which binds and activates Src, and this tyrosine kinase activates PLCγ to increase IP_3. IP3 binds to a receptor/Ca^{2+} channel at the ER to increase $(Ca^{2+})_i$ (Bates et al., 2014; Sato et al., 2006; Stith, 2015). Two different PLD inhibitors prevent the fertilization increase in PA, Src and PLCγ activity, ~87% of the total $(Ca^{2+})_i$ release but only delay the appearance of hot spots (from ~5.6 to 14 min after insemination) and do not change the size of the hot spot. Thus, PA may play a role in an earlier event such as sperm-egg fusion but not generation of the hot spot by sperm. However, PA may induce a mechanism similar to that used by sperm as PA induces hot spots of a similar size, and at a similar time as compared to hot spots induced by sperm (Table 2). This would answer the question of why the global application of PA induced a localized hot spot; like sperm, PA would stimulate a preexisting ER patch with higher levels of IP3 receptor clustering.

4.5. PA induction of a $(Ca^{2+})_i$ wave

Interestingly, the PA-induced hot spots lasted over a half an hour (versus those induced by sperm that up to ~30 s) before a weak and slow $(Ca^{2+})_i$ wave developed. As the wave induced by PA does not accelerate, PA may not be able to induce multiple rotating disks.

Although PA could activate one ER patch or IP_3 receptor to produce a hot spot, the induction of the $(Ca^{2+})_i$ wave by PA may require increased ER patches throughout the egg. While sperm would not require this enhancement to produce a much faster wave, PA may require a half hour after hot spot generation to enhance the ER so that the egg can support a very slow $(Ca^{2+})_i$ wave. This suggestion is based on the fact that PA is involved in membrane bending such as those involved in forming cortical ER patches (see summary in Stith, 2015), and that PA can cause rapid (minutes) ER remodeling in yeast (Carman and Han, 2009). Furthermore, PA is rapidly transferred to the ER by Nir2 (Kim et al., 2015), and PA is elevated during *Xenopus* oocyte maturation to the egg when the cortical ER is forming (Holland et al., 2003). In addition, if PA does enhance ER patching and IP_3 receptor clustering, this is consistent with data showing that PA induced a very slow wave in eggs (much slower than that rapidly induced after PA addition to oocytes; Table 2). As noted, the more IP_3 receptor clustering, the slower the $(Ca^{2+})_i$ wave is: $(Ca^{2+})_i$ released by one IP3 receptor inhibits nearby clustered IP_3 receptors to produce a slow wave (Machaca, 2004).

In experiments contrasting with those involving PA addition, it is important to note that inhibition of PA production by FIPI or 1-butanol actually sped the late fertilization wave by 30% and 15% respectively. As lowering PA did not inhibit the initial speed of the $(Ca^{2+})_i$ wave (thus, not affecting the speed of the initial rotating disk), one would suggest that elevated PA may inhibit the appearance of multiple disks. If true, and PA enhances cortical ER, this may mean that the appearance of multiple rotating disks may be related to ER structure.

Perhaps elevated PA itself does not slow the wave. Without PLD inhibitors, sperm induce a much higher (6.6 fold) increase in $(Ca^{2+})_i$ that would stimulate the metabolism of IP_3 (Stith, 2015; Stith et al., 1994). Thus, the PLD inhibitors could accelerate the wave through abnormal elevation of $[IP_3]$, or the lowering $(Ca^{2+})_i$, to facilitate the appearance of additional rotating disks.

In summary, we suggest that the fertilization $(Ca^{2+})_i$ wave is due to an outwardly rotating disk of elevated $(Ca^{2+})_i$ and that the acceleration of the wave may be due to the appearance of other disks and an acceleration of the disks. We suggest that the initial area of $(Ca^{2+})_i$ release at the sperm-egg binding site (hot spot) may be due to one cortical ER patch with clustered IP_3 receptors. Finally, PA may induce hot spots by a mechanism similar to that used by sperm, and a subsequent $(Ca^{2+})_i$ wave by enhancing IP3 receptor clusters.

Funding sources

Research reported in this publication was 98% supported by Institute of Child Health and Human Development, and Institute of General Medical Sciences of the National Institutes of Health under award numbers R15HD065661-01 and R15GM122036-01 (respectively). The content is solely the responsibility of the authors and does not necessarily represent the official views of the National Institutes of Health. Funding from the Undergraduate Research Opportunity Program, CRISP award and ORS grant at the University of Colorado Denver also supported this work.

References

Bates, R.C., Fees, C.P., Holland, W.L., Winger, C.C., Batbayar, K., Ancar, R., Bergren, T., Petcoff, D., Stith, B.J., 2014. Activation of src and release of intracellular calcium by phosphatidic acid during *Xenopus* laevis fertilization. Dev. Biol. 386, 165–180. http://dx.doi.org/10.1016/j.ydbio.2013.11.006.

Boulware, M.J., Marchant, J.S., 2005. IP3receptor activity is differentially regulated in endoplasmic reticulum subdomains during oocyte maturation. Curr. Biol. 15, 765–770. http://dx.doi.org/10.1016/j.cub.2005.02.065.

Bugrim, A., Fontanilla, R., Eutenier, B.B., Keizer, J., Nuccitelli, R., 2003. Sperm initiate a Ca2+ wave in frog eggs that is more similar to Ca2+ waves initiated by IP3 than by Ca2+. Biophys. J. 84, 1580–1590. http://dx.doi.org/10.1016/S0006-3495(03)74968-6.

Busa, W.B., Ferguson, J.E., Joseph, S.K., Williamson, J.R., Nuccitelli, R., 1985. Activation of frog (*Xenopus* laevis) eggs by inositol trisphosphate. I. Characterization of Ca2+ release from intracellular stores. J. Cell Biol. 101, 677–682.

Campanella, C., Andreuccetti, P., 1977. Ultrastructural observations on cortical endoplasmic reticulum and on residual cortical granules in the egg of *Xenopus* laevis. Dev. Biol. 56, 1–10. http://dx.doi.org/10.1016/0012-1606(77)90150-6.

Carman, G.M., Han, G.S., 2009. Phosphatidic acid phosphatase, a key enzyme in the regulation of lipid synthesis. J. Biol. Chem. 284, 2593–2597. http://dx.doi.org/10.1074/jbc.R800059200.

Carroll, D.J., Ramarao, C.S., Mehlmann, L.M., Roche, S., Terasaki, M., Jaffe, L.A., 1997. Calcium release at fertilization in starfish eggs is mediated by phospholipase Cγ. J. Cell Biol. 138, 1303–1311. http://dx.doi.org/10.1083/jcb.138.6.1303.

Charbonneau, M., Grey, R.D., 1984. The onset of activation responsiveness during maturation coincides with the formation of the cortical endoplasmic reticulum in oocytes of *Xenopus* laevis. Dev. Biol. 102, 90–97. http://dx.doi.org/10.1016/0012-1606(84)90177-5.

Chiba, K., Kado, R.T., Jaffe, L.A., 1990. Development of calcium release mechanisms during starfish oocyte maturation. Dev. Biol. 140, 300–306. http://dx.doi.org/10.1016/0012-1606(90)90080-3.

Dargan, S.L., Parker, I., 2003. Buffer kinetics shape the spatiotemporal patterns of IP3-evoked Ca2+signals. J. Physiol. 553, 775–788. http://dx.doi.org/10.1113/jphysiol.2003.054247.

Darszon, A., Wood, C.D., Beltrán, C., Sánchez, D., Rodríguez, E., Gorelik, J., Korchev, Y.E., Nishigaki, T., 2004. Measuring ion fluxes in sperm. Methods Cell Biol. 74, 545–576. http://dx.doi.org/10.1016/S0091-679X(04)74022-4.

El-Jouni, W., Jang, B., Haun, S., Machaca, K., 2005. Calcium signaling differentiation during *Xenopus* oocyte maturation. Dev. Biol. 288, 514–525. http://dx.doi.org/10.1016/j.ydbio.2005.10.034.

Fall, C.P., Wagner, J.M., Loew, L.M., Nuccitelli, R., 2004. Cortically restricted production of IP3leads to propagation of the fertilization Ca2+wave along the cell surface in a model of the *Xenopus* egg. J. Theor. Biol. 231, 487–496. http://dx.doi.org/10.1016/j.jtbi.2004.06.019.

Fontanilla, R.A., Nuccitelli, R., 1998. Characterization of the sperm-induced calcium wave in *Xenopus* eggs using confocal microscopy. Biophys. J. 75, 2079–2087. http://dx.doi.org/10.1016/S0006-3495(98)77650-7.

Girard, S., Lückhoff, A., Lechleiter, J., Sneyd, J., Clapham, D., 1992. Two-dimensional model of calcium waves reproduces the patterns observed in *Xenopus* oocytes. Biophys. J. 61, 509–517. http://dx.doi.org/10.1016/S0006-3495(92)81855-6.

Glahn, D., Mark, S.D., Behr, R.K., Nuccitelli, R., 1999. Tyrosine kinase inhibitors block sperm-induced egg activation in *Xenopus* laevis. Dev. Biol. 205, 171–180. http://dx.doi.org/10.1006/dbio.1998.9042.

Holland, W.L., Stauter, E.C., Stith, B.J., 2003. Quantification of phosphatidic acid and lysophosphatidic acid by HPLC with evaporative light-scattering detection. J. Lipid Res. 44, 854–858. http://dx.doi.org/10.1194/jlr.D200040-JLR200.

Kim, Y.J., Guzman-Hernandez, M.L., Wisniewski, E., Balla, T., 2015. Phosphatidylinositol-phosphatidic acid exchange by Nir2 at ER-PM contact sites

maintains phosphoinositide signaling competence. Dev. Cell 33, 549–561. http://dx.doi.org/10.1016/j.devcel.2015.04.028.
Kline, D., 2000. Attributes and dynamics of the endoplasmic reticulum in mammalian eggs. Curr. Top. Dev. Biol. 50, 125–154. http://dx.doi.org/10.1016/S0070-2153(00)50007-6.
Larabell, C., Nuccitelli, R., 1992. Inositol lipid hydrolysis contributes to the Ca2+wave in the activating egg of *Xenopus* laevis. Dev. Biol. 153, 347–355. http://dx.doi.org/10.1016/0012-1606(92)90119-2.
Lechleiter, J., Girard, S., Peralta, E., Clapham, D., 1991. Spiral calcium wave propagation and annihilation in *Xenopus* laevis oocytes. Science 252 (80), 123–126. http://dx.doi.org/10.1126/science.2011747.
Machaca, K., 2004. Increased sensitivity and clustering of elementary Ca2+release events during oocyte maturation. Dev. Biol. 275, 170–182. http://dx.doi.org/10.1016/j.ydbio.2004.08.004.
Nuccitelli, R., Yim, D.L., Smart, T., 1993. The sperm-induced Ca2+wave following fertilization of the *Xenopus* egg requires the production of ins(1,4,5)P3. Dev. Biol. 158, 200–212. http://dx.doi.org/10.1006/dbio.1993.1179.
Runft, L.L., Watras, J., Jaffe, L.A., 1999. Calcium release at fertilization of *Xenopus* eggs requires type I IP3receptors, but not SH2 domain-mediated activation of PLCγ or G(q)-mediated activation of PLCβ. Dev. Biol. 214, 399–411. http://dx.doi.org/10.1006/dbio.1999.9415.
Sato, K. ichi, Fukami, Y., Stith, B.J., 2006. Signal transduction pathways leading to Ca2+release in a vertebrate model system: Lessons from *Xenopus* eggs. Semin. Cell Dev. Biol. 17, 285–292. http://dx.doi.org/10.1016/j.semcdb.2006.02.008.
Sato, K.I., Iwao, Y., Fujimura, T., Tamaki, I., Ogawa, K., Iwasaki, T., Tokmakov, A.A., Hatano, O., Fukami, Y., 1999. Evidence for the involvement of a Src-related tyrosine kinase in *Xenopus* egg activation. Dev. Biol. 209, 308–320. http://dx.doi.org/10.1006/dbio.1999.9255.
Shuai, J., Pearson, J.E., Foskett, J.K., Mak, D.O.D., Parker, I., 2007. A kinetic model of single and clustered IP3 receptors in the absence of Ca2+ feedback. Biophys. J. 93, 1151–1162. http://dx.doi.org/10.1529/biophysj.107.108795.
Shuai, J., Rose, H.J., Parker, I., 2006. The number and spatial distribution of IP3 receptors underlying calcium puffs in *Xenopus* oocytes. Biophys. J. 91, 4033–4044. http://dx.doi.org/10.1529/biophysj.106.088880.
Stith, B., Woronoff, K., Espinoza, R., Smart, T., 1997. sn-1,2-diacylglycerol and choline increase after fertilization in *Xenopus* Iaevis. Mol. Biol. Cell 8, 755–765. http://dx.doi.org/10.1091/mbc.8.4.755.
Stith, B.J., 2015. Phospholipase C and D regulation of Src, calcium release and membrane fusion during *Xenopus* laevis development. Dev. Biol.. http://dx.doi.org/10.1016/j.ydbio.2015.02.020.
Stith, B.J., Espinoza, R., Roberts, D., Smart, T., 1994. Sperm increase inositol 1,4,5-trisphosphate mass in *Xenopus* laevis eggs preinjected with calcium buffers or heparin. Dev. Biol. 165, 206–215. http://dx.doi.org/10.1006/dbio.1994.1247.
Stith, B.J., Goalstone, M., Silva, S., Jaynes, C., 1993. Inositol 1,4,5-trisphosphate mass changes from fertilization through first cleavage in *Xenopus* laevis. Mol. Biol. Cell, 4. http://dx.doi.org/10.1091/mbc.4.4.435.
Stith, B.J., Goalstone, M.L., Kirkwood, A.J., 1992. Protein kinase C initially inhibits the induction of meiotic cell division in *Xenopus* oocytes. Cell. Signal. 4, 393–403. http://dx.doi.org/10.1016/0898-6568(92)90034-6.
Stricker, S.A., 2006. Structural reorganizations of the endoplasmic reticulum during egg maturation and fertilization. Semin. Cell Dev. Biol.. http://dx.doi.org/10.1016/j.semcdb.2006.02.002.
Stricker, S.A., Carroll, D.J., Tsui, W.L., 2010. Roles of Src family kinase signaling during fertilization and the first cell cycle in the marine protostome worm Cerebratulus. Int. J. Dev. Biol. 54, 787–793. http://dx.doi.org/10.1387/ijdb.092918ss.
Sun, L., Yu, F., Ullah, A., Hubrack, S., Daalis, A., Jung, P., Machaca, K., 2011. Endoplasmic reticulum remodeling tunes IP3-dependent Ca2+release sensitivity. PLoS One, 6. http://dx.doi.org/10.1371/journal.pone.0027928.
Terasaki, M., Runft, L.L., Hand, A.R., 2001. Changes in organization of the endoplasmic reticulum during *Xenopus* oocyte maturation and activation. Mol. Biol. Cell 12, 1103–1116. http://dx.doi.org/10.1091/mbc.12.4.1103.
Ullah, A., Jung, P., Ullah, G., Machaca, K., 2014. The role of IP3Receptor channel clustering in Ca2 +wave propagation during oocyte maturation. Prog. Mol. Biol. Transl. Sci. 123, 83–101. http://dx.doi.org/10.1016/B978-0-12-397897-400006-1.
Wagner, J., Fall, C.F., Hong, F., Sims, C.E., Allbritton, N.L., Fontanilla, R.A., Moraru, I.I., Loew, L.M., Nuccitelli, R., 2004. A wave of IP3production accompanies the fertilization Ca2+wave in the egg of the frog, *Xenopus* laevis: theoretical and experimental support. Cell Calcium 35, 433–447. http://dx.doi.org/10.1016/j.ceca.2003.10.009.
Wagner, J., Li, Y.X., Pearson, J., Keizer, J., 1998. Simulation of the fertilization Ca2+ wave in *Xenopus* laevis eggs. Biophys. J. 75, 2088–2097. http://dx.doi.org/10.1016/S0006-3495(98)77651-9.
Wozniak, K.L., Phelps, W.A., Tembo, M., Lee, M.T., Carlson, A.E., 2018. The TMEM16A Mediates the Fast Polyspermy block in *Xenopus* Laevis. J. Gen. Physiol. 112. http://dx.doi.org/10.1016/j.bpj.2016.11.2978, (552a–552a).